

Firefly Algorithm-based Optimization of Control Parameters in DC Conversion Systems

Thanh-Lam Le

Faculty of Electrical and Electronics Engineering, Ho Chi Minh City University of Technology and Education, Vietnam

lamlethanh@hcmute.edu.vn (corresponding author)

Received: 13 November 2024 | Revised: 17 December 2024 | Accepted: 1 January 2025

Licensed under a CC-BY 4.0 license | Copyright (c) by the authors | DOI: <https://doi.org/10.48084/etasr.9606>

ABSTRACT

Sustainable energy and electric vehicles require DC-DC converters in renewable energy systems, EV charging, and smart grids. In this context, buck converters are crucial, providing efficient voltage regulation and reliable performance in these advanced energy systems. While Proportional-Integral (PI) controllers are widely adopted for their simplicity and dependability, they often rely on manual parameter tuning, limiting their adaptability and responsiveness. To address this limitation, this research introduces a digital control strategy that optimizes the PI parameters using the Firefly Algorithm (FA). This optimization significantly enhances the stability and reduces the oscillations in the DC-DC buck converter. A MATLAB/Simulink simulation model is utilized to validate the proposed approach, and the results demonstrate that the FA-optimized control parameters substantially improve the converter's performance, making it highly suitable for high-demand applications in advanced energy systems.

Keywords-converter system; meta-heuristic algorithm; firefly algorithm; voltage regulation

I. INTRODUCTION

The global transition toward sustainable energy and the rapid expansion of electric vehicles have made DC-DC converters essential components in modern power systems, providing critical voltage regulation for a variety of applications [1, 2]. These converters are vital in adjusting voltage levels to accommodate renewable energy sources, like solar and wind, electric vehicle charging infrastructure, and smart home systems [3, 4]. As power networks become increasingly decentralized, DC-DC converters enable reliable and efficient power management, maintaining stable outputs despite the fluctuations in load and input supply—a capability particularly crucial in microgrids, where energy demands and sources vary dynamically [5]. Additionally, recent advancements in control strategies have improved the performance and adaptability of DC-DC converters, enhancing their efficiency, power density, and cost-effectiveness. These converters rely on configurations, such as buck, boost, and cuk, to meet the specific requirements of low-voltage applications, which renders them indispensable in the next-generation energy systems, prioritizing resilience and environmental sustainability [6, 7]. However, designing converters that consistently provide stable voltage output poses significant challenges, as the input voltage, load demands, and circuit parameters can widely fluctuate [8]. To address these issues, advanced control strategies, including adaptive and neural network-based methods, have been developed to enhance the converter performance and reliability under changing conditions [9-11]. Yet, the growing complexity of these systems, with more sophisticated control mechanisms, can

increase the production costs and hinder scalability for commercial use [12-14]. Ongoing research seeks to develop adaptable, resilient, and sustainable DC-DC converters that balance advanced functionality with economic feasibility, addressing the demands of modern power systems while supporting industrial scalability and a widespread adoption.

In open-loop configurations, achieving a stable output in buck converters with a fixed duty cycle is challenging due to the nonlinear characteristics of the circuit components [15]. To address these challenges, feedback loops are widely employed to ensure consistent voltage regulation by rapidly adapting to changes in operating conditions [16]. Recent advancements in digital control have further refined the buck converter performance, offering benefits, like faster switching speeds and easier integration with microcontrollers, such as Digital Signal Processors (DSPs) [17]. This digital control approach enhances stability, reduces response times, and aligns with the stringent requirements of the modern, high-efficiency applications. PI control is a cornerstone in power conversion systems, valued for its straightforward design, reliability, and effectiveness in stabilizing the output voltage. Commonly utilized in buck converters, PI controllers offer dependable steady-state performance and swift transient response, even as the load and input conditions fluctuate [18]. Their design simplicity demands minimal computational power, making them well-suited for integration into microcontroller-based applications, where cost and resource efficiency are critical. Despite these benefits, the PI controller often relies on manually tuned parameters, proportional gain (K_p), and integral gain (K_i), which are typically set through empirical methods or

trial and error [19]. This approach can fall short, potentially causing slower response, increased steady-state error, or even instability in varying operational scenarios [20]. Furthermore, fixed PI settings may lack the adaptability needed to handle the dynamic changes in the system load or input [21-23]. These limitations emphasize the need for parameter optimization to allow PI controllers to dynamically adapt to and ensure stability in DC-DC converter systems.

This study focuses on optimizing the control parameters for the DC-DC buck converters using the FA to enhance performance and stability. Conventional DC-DC energy conversion systems often encounter instability and oscillations due to the changing loads or input voltages, posing challenges for maintaining minimal ripple and noise, especially in applications, like medical devices, military equipment, or signal processing electronics. To address these issues, this research employs a digital control method where PI controller parameters are dynamically tuned using FA. By leveraging this optimization technique, the converter's responsiveness and stability are significantly improved. A simulation model of the DC-DC buck converter was developed and analyzed in the MATLAB/Simulink environment to validate the proposed approach. The results demonstrate the efficiency and robustness of the FA-optimized PI controller in achieving reliable step-down energy conversion, making it suitable for high-performance applications.

II. SYSTEM ANALYSIS

A typical buck converter comprises a DC input voltage source (V_{in}), a controllable switch (S_w), a diode (D), an inductor (L) for current smoothing, a capacitor (C) for voltage filtering, and a load resistor (R), as illustrated in Figure 1. The converter operates by switching between two distinct states, ON and OFF, each described by unique equations that characterize the system's dynamics at each phase. These equations provide a framework for accurately analyzing the buck converter's performance across different operating conditions, highlighting its efficiency and stability in voltage regulation. The system model in a state-space form is expressed using:

$$\begin{cases} \frac{di_L}{dt} = \frac{1}{L}(V_{in} - v_o) \\ \frac{dv_o}{dt} = \frac{1}{C}(i_L - \frac{v_o}{R}) \\ \frac{di_L}{dt} = -\frac{v_o}{L} \end{cases} \quad (1)$$

Combining the equations in (1) yields the ones shown in (2):

$$\begin{cases} \frac{di_L}{dt} = \frac{1}{L}(uV_{in} - v_o) \\ \frac{dv_o}{dt} = \frac{1}{C}(i_L - \frac{v_o}{R}) \end{cases} \quad (2)$$

where u represents the control input, taking a value of 1 when the switch is ON and 0 when it is OFF. The output voltage error and its rate of change, indicating how the output voltage error evolves over time, are defined as $x_1 = v_o - V_{ref}$ and $x_2 = \dot{v}_o - \dot{V}_{ref} = \dot{x}_1 = \dot{v}_o$, where \dot{x}_1 represents the derivative

of x_1 , and V_{ref} denotes the target DC reference value for the output voltage.

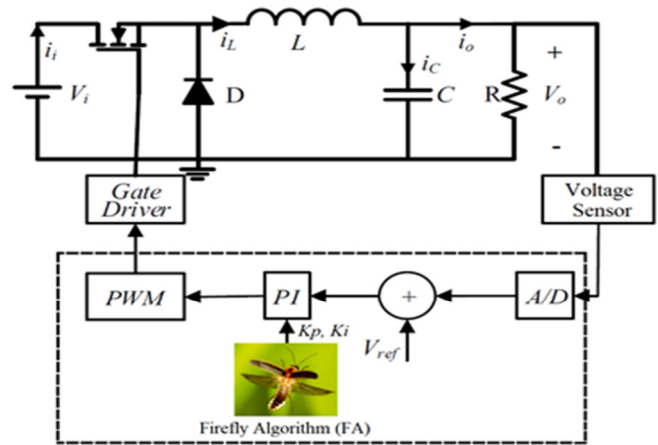


Fig. 1. Block diagram overview of DC-DC converter system integrated with FA.

By differentiating the output voltage v_o in (2) with respect to time, the output voltage error x_1 and its rate of change x_2 is expressed as:

$$\begin{cases} \dot{x}_1 = x_2 \\ \dot{x}_2 = -\frac{\dot{x}_1}{RC} + \omega_0^2(uV_{in} - V_{ref} - x_1) \\ \omega_0^2 = \frac{1}{LC} \end{cases} \quad (3)$$

The current flow in a buck converter operating in Continuous Conduction Mode (CCM) is determined by the switch S_w . When switch is ON, the diode is reverse-biased, and the input supplies power to both the load and the inductor, causing the inductor current to increase over the interval DT . When S_w turns OFF, the inductor voltage reverses, and the current continues to flow through the diode during $(1-D)$. Under steady-state conditions, the average inductor current equals the average output current, as the capacitor's average current remains zero. The relationship between the input voltage V_i and output voltage V_o , governed by the duty cycle D and switching period T , is given by $V_o = D \cdot V_{in}$ where $D = \frac{t_{on}}{T}$. The variable t_{on} represents the period during which the switch remains in the ON state. There is a direct proportional relationship between the output and input voltages, governed by the duty cycle ($0 < D < 1$). Since the duty cycle is always less than 1, the output voltage remains consistently lower than the input voltage.

III. VOLTAGE REGULATION TECHNIQUE

Achieving stable output voltage in a buck converter with a fixed duty cycle is especially challenging in open-loop configurations, particularly when exposed to load fluctuations or external disturbances. To address this, a feedback loop is necessary to regulate the output voltage dynamically as conditions change. Figure 1 presents the block diagram of a digital PI-controlled buck converter operating in voltage mode, incorporating both power stages and feedback elements.

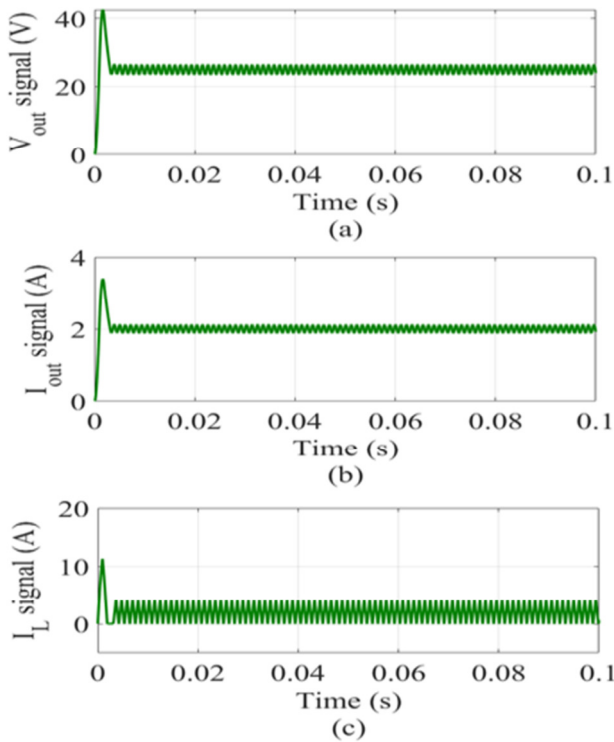


Fig. 2. Analysis of simulation results for (a) V_{outs} , (b) I_{outs} , and (c) I_L without using FA, at an output reference voltage of 25 V DC.

A voltage sensor is used to capture the output voltage (V_0) from the converter, which is then processed through a signal conditioning circuit to match the input requirements of the analog channel, ultimately interfacing with the DSP. The converter's output is compared to a reference voltage (V_{ref}), and the resulting error is minimized through the PI controller. The PI controller output modulates the duty cycle in the Pulse Width Modulation (PWM) module, which then generates a pulse signal for digital-to-analog conversion. This pulse signal directly controls the semiconductor switch, turning it on and off through the driver circuit. The closed-loop controller is engineered to align the output voltage (V_0) closely with the desired reference voltage (V_{ref}). PI control is a popular choice in buck converters because of its straightforward implementation and cost-effectiveness. The PI control signal is mathematically expressed by:

$$u(t) = K_p e(t) + K_i \int_0^t e(\tau) d\tau \quad (4)$$

In digitally controlled switch-mode power supplies, the control signal $u(t)$ and error signal $e(t)$, defined in (4), are critical for regulating performance, with the K_p and K_i gains adjusting the response. The proportional term minimizes the error by applying a gain to the error, though high K_p values can induce output fluctuations and risk destabilization. Conversely, low K_p values slow the response to input disturbances, while the integral term, through K_i , accumulates the error over time to correct residual inaccuracies. Together, these parameters enable an accurate regulation, as the closed-loop converter's performance heavily depends on them. Microcontrollers

generate the PWM signals, essential for switching, but the low output voltage requires an intermediary circuit to boost it for effective switching. This circuit not only enables rapid switching and reduces energy loss, but also protects the microcontroller from voltage spikes and offload dissipation, thereby enhancing system durability and efficiency.

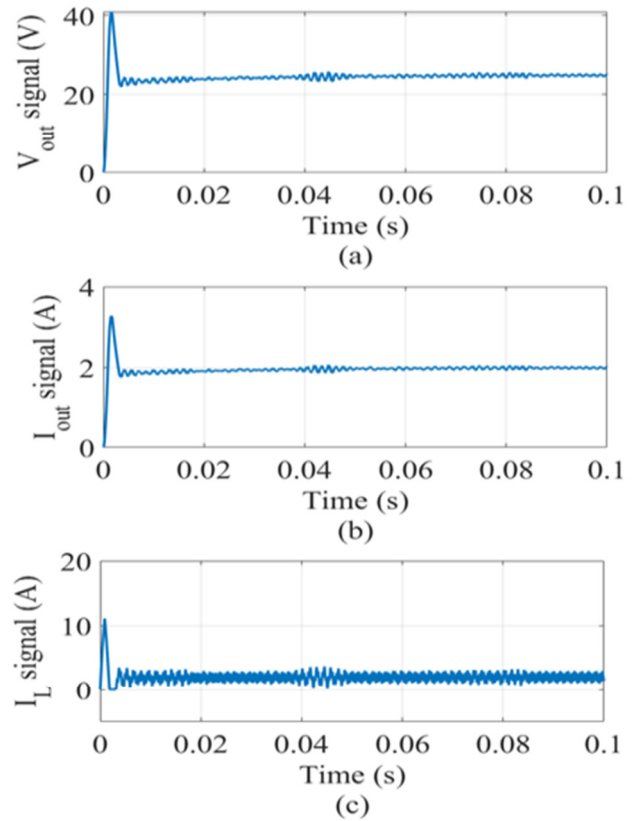


Fig. 3. Analysis of simulation results for (a) V_{outs} , (b) I_{out} , and (c) I_L with FA optimization, at an output reference voltage of 25 V DC.

Figures 2 and 3 present the simulation results comparing the effectiveness of the FA in optimizing the control parameters. They illustrate the analysis results without and with the application of the FA optimization technique, respectively, for the case where the reference voltage is set to 25 V DC. Initially, Figure 2 depicts the performance of the DC buck converter system with the PI parameters having been empirically set at $K_p = 50$ and $K_i = 0.5$. As shown in Figure 2(a), the output voltage closely tracks the reference value of 25 V DC, achieving a settling time of 0.003 s. Figures 2(b) and 2(c) display the load and inductor currents, respectively, both stabilizing quickly without a notable overshoot or prolonged transients. These results confirm the effectiveness of the closed-loop digital control approach for the step-down energy conversion systems. Although satisfactory results are obtained, the controller parameters are not fully optimized, impacting the converter's overall control quality and efficiency. Consequently, the FA is employed to optimize the PI parameters, refining them to $K_p = 0.27$ and $K_i = 9.24$ after two iterations. Figure 3 portrays the improved performance

with the optimized control parameters, showing a more precise output voltage with reduced oscillations and overshoot in both voltage and current, compared to the non-optimized settings.

IV. FA FOR PI OPTIMIZATION

The FA is a metaheuristic optimization technique that draws inspiration from the natural bioluminescent signaling behavior of fireflies. It is specifically designed to address complex, multimodal optimization problems [24, 25]. In the FA, each firefly represents a candidate solution, with its "brightness" indicating the quality of the solution as evaluated by a fitness function. Fireflies are attracted to others with higher brightness, causing less optimal solutions to move toward more optimal ones. Through this interactive process, the population of fireflies progressively converges toward the global optimum over multiple iterations. A key strength of the FA is its ability to effectively explore a broad search space, making it particularly suitable for problems with numerous local optima.

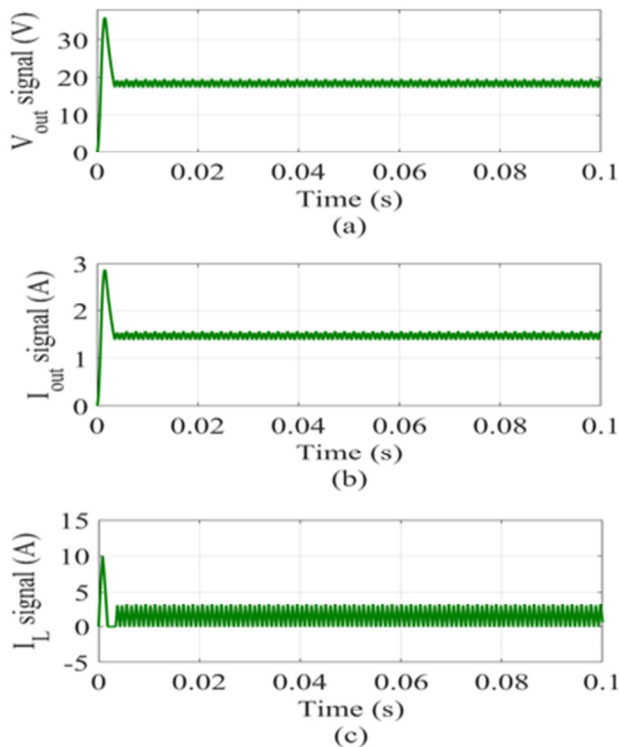


Fig. 4. Analysis of simulation results for (a) V_{out} , (b) I_{out} , and (c) I_L without using FA, at an output reference voltage of 18 V DC.

By fine-tuning the light absorption and attraction parameters, the FA can maintain an equilibrium between exploration and exploitation, thereby mitigating the risk of premature convergence during the optimization process. Compared to other algorithms, such as Particle Swarm Optimization (PSO) and Genetic Algorithms (GA), the FA stands out for its simplicity, flexibility, and ease of implementation [24]. Its ability to precisely adjust parameters makes it particularly effective for optimizing the PI controller parameters, where accurate tuning is crucial for achieving

optimal control performance. The FA operates using key mathematical expressions that govern the movement of fireflies toward brighter, more optimal solutions within the search space. The attractiveness of a firefly, denoted as $\beta(r)$, diminishes as the distance, denoted as r , between two fireflies increases, reflecting the natural phenomenon where light intensity diminishes with distance. Mathematically, the attractiveness is expressed as:

$$\beta(r) = \beta_0 e^{-\gamma r^2} \quad (5)$$

where β_0 represents the maximum attractiveness when $r = 0$, and γ is the light absorption coefficient, which controls how quickly attractiveness decreases with distance.

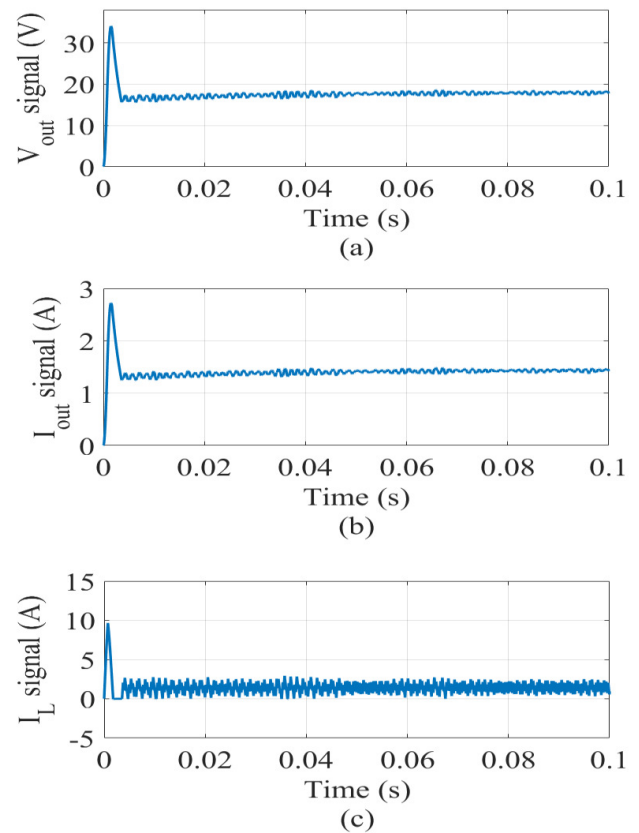


Fig. 5. Analysis of simulation results for (a) V_{out} , (b) I_{out} , and (c) I_L with FA optimization, at an output reference voltage of 18 V DC.

This aforementioned mechanism enables the FA to balance exploration and exploitation, as fireflies are attracted to brighter solutions while still exploring the search space effectively. By adjusting parameters, like γ and β_0 , the FA can adapt to different optimization problems, ensuring convergence to high-quality solutions. The distance r_{ij} between any two fireflies i and j , located at positions x_i and x_j , respectively, is calculated using the Euclidean distance formula:

$$r_{ij} = \sqrt{\sum_{k=1}^d (x_{i,k} - x_{j,k})^2} \quad (6)$$

where d is the dimensionality of the solution space. To simulate movement, each firefly i is drawn toward a brighter firefly j through:

$$x_i = x_i + \beta_0 e^{-\gamma r_{ij}^2} (x_j - x_i) + \alpha (\text{rand} - 0.5) \quad (7)$$

where the first term models the attraction component, while the last term introduces random perturbations, with α being utilized as the randomization parameter and rand as a uniformly distributed random variable. Together, these expressions enable the FA to balance exploration and exploitation, guiding the population toward optimal solutions in complex optimization landscapes.

The test results with a reference voltage of 18 V DC are presented in Figures 4 and 5. Once again, the results demonstrate that the output quality of the DC-DC converter is well-maintained when the optimization of the controller parameters is applied, as shown in Figure 5. In contrast, without the optimization of the controller parameters, the PI controller can still regulate the output to track the reference voltage. However, its performance does not reach the same level of efficiency, as depicted in Figure 4.

To provide a structured guideline on using the FA for optimizing the PI controller parameters, the following pseudo code and explanation offer a step-by-step approach for implementing FA in this specific context. By iteratively adjusting the PI parameters, FA guides the solutions toward an optimal configuration. The process is outlined as follows with the objective function $f(x)$, where $x = (K_p, K_i)$:

1. Generate initial population: Generate an initial population of fireflies x_i for $i = 1, 2, \dots, n$, each with random values for K_p and K_i .
2. Evaluate brightness or light intensity: Calculate the light intensity I_i at each firefly position x_i using the objective function $f(x_i)$, which reflects the fitness or quality of the PI parameters.
3. Define light absorption coefficient: Set the light absorption coefficient γ , which controls how quickly attractiveness decreases with distance.
4. Optimization Loop: While $t < \text{MaxIt}$, where MaxIt is the maximum number of iterations, for each firefly $i = 1:n$ and for each other firefly $j = 1:n$ we check if $I_j > I_i$, indicating firefly j has a better solution. If the previous condition is true then:
 - a. Move firefly i towards firefly j in the 2-dimensional space of K_p and K_i .
 - b. The attractiveness decreases with distance r according to $\exp(-\gamma \cdot r)$.
 - c. Evaluate the new position of firefly i and update its light intensity I_i .
 - d. End inner loop for j .
 - e. End outer loop for i .

- f. Rank the fireflies and identify the current best solution.
- g. Gradually reduce the mutation coefficient α to balance exploration and exploitation.
- h. End while loop.

5. Post-Process Results: After completing the iterations, identify the optimal values for K_p and K_i from the best-performing firefly.
6. Update and Visualize: Update the Simulink model with the optimized K_p and K_i values. Visualize the convergence of the best cost over iterations to evaluate the optimization process.

V. ANALYSIS RESULTS

For this analysis, the input voltage is fixed at 50V DC, while the target output voltage is examined under two conditions: 25 V DC and 18V DC, respectively. The carrier frequency is specified at 2.5 kHz. The key parameters of the FA are selected as follows: d is 2, MaxIt is set to 2, the population size or number of fireflies is 10, γ is set to 1, β_0 referring to the base attraction coefficient is set to 2, and α is chosen as 0.2.

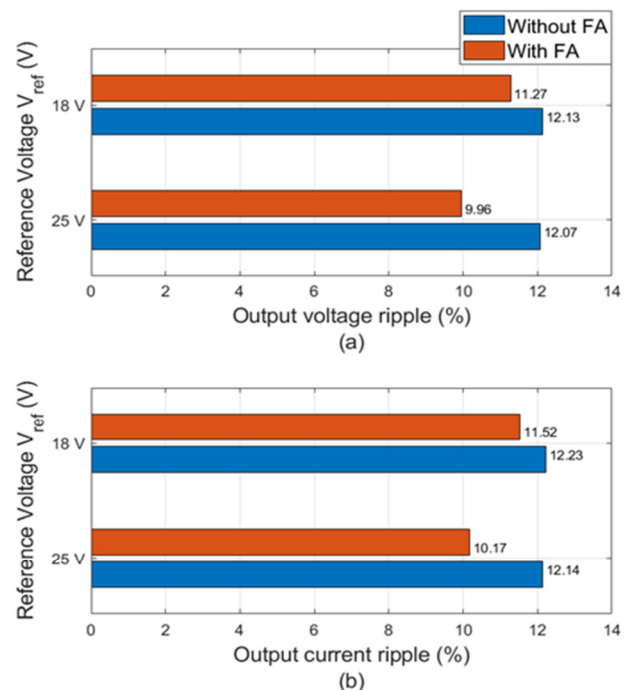


Fig. 6. Comparison of ripple percentage of output voltage and output current with and without FA optimization at different set voltages: (a) output voltage ripple and (b) output current ripple.

The comparison of the ripple percentage of the output voltage and output current with and without FA optimization at different set voltages is presented in Figure 6. As observed, the ripple percentage of both current and voltage is significantly reduced when the FA-based controller parameter optimization

is applied. The ripple percentage values are calculated according to the method described in [8]. Thus, applying optimization techniques like FA enhances the output quality in DC buck converters without redesigning the circuit or adding additional passive elements, effectively reducing costs while improving system performance.

VI. CONCLUSION

This study describes an advanced digital control technique for optimizing the PI controller parameters in DC-DC buck converters utilizing the Firefly Algorithm (FA). By addressing the limitations of conventional manual parameter tuning, the proposed approach significantly enhances the stability and performance of the converter under varying conditions. The simulation results, conducted in the MATLAB/Simulink environment, validate that the FA-optimized PI parameters effectively mitigate oscillations and output ripple, thereby ensuring an improved dynamic response and robust operation. The proposed method is particularly beneficial for high-performance applications in advanced energy systems, such as renewable energy systems, electric vehicle charging, and smart grids, where reliable voltage regulation is critical. The FA-based optimization does not require additional circuit modifications or passive components, rendering it a cost-effective and scalable solution. As the demand for efficient energy conversion continues to rise, this research highlights the potential of intelligent control strategies to improve converter adaptability and responsiveness, meeting the requirements of the modern energy applications.

REFERENCES

- [1] Z. R. Labidi, H. Schulte, and A. Mami, "A Model-Based Approach of DC-DC Converters Dedicated to Controller Design Applications for Photovoltaic Generators," *Engineering, Technology & Applied Science Research*, vol. 9, no. 4, pp. 4371–4376, Aug. 2019, <https://doi.org/10.48084/etasr.2829>.
- [2] D. K. Dhaked, Y. Gopal, and D. Birla, "Battery Charging Optimization of Solar Energy based Telecom Sites in India," *Engineering, Technology & Applied Science Research*, vol. 9, no. 6, pp. 5041–5046, Dec. 2019, <https://doi.org/10.48084/etasr.3121>.
- [3] V.-Q. Nguyen and T.-L. Le, "Flexible Control with Fuzzy Observer-Based Sliding mode for Multilevel Inverter," *Journal of Electrical Engineering & Technology*, vol. 19, no. 7, pp. 4573–4586, Mar. 2024, <https://doi.org/10.1007/s42835-024-01878-9>.
- [4] A. Nouaiti, M. Reddak, C. Boutahiri, A. Mesbahi, A. M. Hsaini, and A. Bouazi, "A Single Stage Photovoltaic Solar Pumping System based on the Three Phase Multilevel Inverter," *Engineering, Technology & Applied Science Research*, vol. 13, no. 6, pp. 12145–12150, Dec. 2023, <https://doi.org/10.48084/etasr.6403>.
- [5] S. Ansari, A. Chandel, and M. Tariq, "A Comprehensive Review on Power Converters Control and Control Strategies of AC/DC Microgrid," *IEEE Access*, vol. 9, pp. 17998–18015, 2021, <https://doi.org/10.1109/ACCESS.2020.3020035>.
- [6] A. Zentani, A. Almaktoof, and M. T. Kahn, "A Comprehensive Review of Developments in Electric Vehicles Fast Charging Technology," *Applied Sciences*, vol. 14, no. 11, May 2024, Art. no. 4728, <https://doi.org/10.3390/app14114728>.
- [7] D. Mathew and R. C. Naidu, "Investigation of single-stage transformerless buck-boost microinverters," *IET Power Electronics*, vol. 13, no. 8, pp. 1487–1499, 2020, <https://doi.org/10.1049/iet-pel.2019.1237>.
- [8] T.-L. Le and M.-F. Hsieh, "An enhanced direct torque control strategy with composite controller for permanent magnet synchronous motor," *Asian Journal of Control*, vol. 26, no. 4, pp. 1683–1702, Jan. 2024, <https://doi.org/10.1002/asjc.3306>.
- [9] S. Srinivasan, R. Tiwari, M. Krishnamoorthy, M. P. Lalitha, and K. K. Raj, "Neural network based MPPT control with reconfigured quadratic boost converter for fuel cell application," *International Journal of Hydrogen Energy*, vol. 46, no. 9, pp. 6709–6719, Feb. 2021, <https://doi.org/10.1016/j.ijhydene.2020.11.121>.
- [10] V.-Q. Nguyen, M.-T. Nguyen, T.-L. Le, and N.-B. Nguyen, "Current Control for Multi-Level Inverters Based on Fuzzy Logic Sliding Mode Control Approach," in *Proceedings of International Conference on System Science and Engineering*, Ho Chi Minh, Vietnam, Jul. 2023, pp. 444–449, <https://doi.org/10.1109/ICSSE58758.2023.10227186>.
- [11] Y. Gao, S. Wang, T. Dragicevic, P. Wheeler, and P. Zanchetta, "Artificial Intelligence Techniques for Enhancing the Performance of Controllers in Power Converter-Based Systems—An Overview," *IEEE Open Journal of Industry Applications*, vol. 4, pp. 366–375, 2023, <https://doi.org/10.1109/OJIA.2023.3338534>.
- [12] R. Sambath and T. selvaraj, "Enhanced grid stability in PV systems using an improved Luo converter and neural network-based droop control," *Electrical Engineering*, Sep. 2024, <https://doi.org/10.1007/s00202-024-02744-7>.
- [13] T. A. Trivedi, R. Jadeja, and P. Bhatt, "A Review on Direct Power Control for Applications to Grid Connected PWM Converters," *Engineering, Technology & Applied Science Research*, vol. 5, no. 4, pp. 841–849, Aug. 2015, <https://doi.org/10.48084/etasr.544>.
- [14] T.-L. Le and V.-Q. Nguyen, "A Robust Control for Five-level Inverter Based on Integral Sliding Mode Control," *International Journal of Integrated Engineering*, vol. 15, no. 4, pp. 177–192, Oct. 2023, <https://doi.org/10.30880/ijie.2023.15.04.016>.
- [15] S. Mohamadian and M. H. Khanzade, "A Five-Level Current-Source Inverter for Grid-Connected or High-Power Three-Phase Wound-Field Synchronous Motor Drives," *Engineering, Technology & Applied Science Research*, vol. 6, no. 5, pp. 1139–1148, Oct. 2016, <https://doi.org/10.48084/etasr.695>.
- [16] T.-L. Le, M.-F. Hsieh, P.-T. Nguyen, and M.-T. Nguyen, "Speed Control for Permanent Magnet Synchronous Motor Based on Terminal Sliding Mode High-order Control," in *Proceedings of International Conference on System Science and Engineering*, Ho Chi Minh, Vietnam, Jul. 2023, pp. 496–501, <https://doi.org/10.1109/ICSSE58758.2023.10227245>.
- [17] J. Camacho, L. Ibarra, and P. Ponce, "Evaluating the Influence of Execution Speed on Real-Time Simulation Accuracy: a Buck Converter Case Study," *IEEE Access*, 2024, <https://doi.org/10.1109/ACCESS.2024.3452048>.
- [18] M. Jabari, D. Izci, S. Ekinci, M. Bajaj, and I. Zaitsev, "Performance analysis of DC-DC Buck converter with innovative multi-stage PIDn(1+PD) controller using GEO algorithm," *Scientific Reports*, vol. 14, no. 1, Oct. 2024, Art. no. 25612, <https://doi.org/10.1038/s41598-024-77395-6>.
- [19] T.-L. Le and M.-F. Hsieh, "A sliding mode-based single-loop control strategy for permanent magnet synchronous motor drives," *IET Power Electronics*, vol. 17, no. 1, pp. 78–91, Nov. 2023, <https://doi.org/10.1049/pel2.12616>.
- [20] H. Li, B. Song, T. Chen, Y. Xie, and X. Zhou, "Adaptive fuzzy PI controller for permanent magnet synchronous motor drive based on predictive functional control," *Journal of the Franklin Institute*, vol. 358, no. 15, pp. 7333–7364, Oct. 2021, <https://doi.org/10.1016/j.jfranklin.2021.07.024>.
- [21] T.-L. Le, M.-F. Hsieh, and M.-T. Nguyen, "Robust Speed Control With Disturbance Rejection for Surface-mounted Permanent Magnet Synchronous Motor," in *Proceedings of 6th International Conference on Green Technology and Sustainable Development*, Nha Trang City, Vietnam, Jul. 2022, pp. 459–463, <https://doi.org/10.1109/GTSD54989.2022.9989278>.
- [22] N. Chettibi and A. Mellit, "Intelligent control strategy for a grid connected PV/SOFC/BESS energy generation system," *Energy*, vol. 147, pp. 239–262, Mar. 2018, <https://doi.org/10.1016/j.energy.2018.01.030>.
- [23] F. Liu, W. Liu, and H. Luo, "Operational stability control of a buried pipeline maintenance robot using an improved PSO-PID controller,"

- Tunnelling and Underground Space Technology*, vol. 138, Aug. 2023, Art. no. 105178, <https://doi.org/10.1016/j.tust.2023.105178>.
- [24] X.-S. Yang, "Firefly Algorithms for Multimodal Optimization," in *Stochastic Algorithms: Foundations and Applications*, Sapporo, Japan, 2009, pp. 169–178, https://doi.org/10.1007/978-3-642-04944-6_14.
- [25] J. Zhao, S. Lv, R. Xiao, H. Ma, and J.-S. Pan, "Hierarchical learning multi-objective firefly algorithm for high-dimensional feature selection," *Applied Soft Computing*, vol. 165, Nov. 2024, Art. no. 112042, <https://doi.org/10.1016/j.asoc.2024.112042>.